Progress In Electromagnetics Research C, Vol. 122, 41–56, 2022

Design of Capacitive Coupled Log Periodic Dielectric Resonator Antenna for X Band Applications

Boddapallli V. Ramana[1, *], Prudhivi Mallikarjuna Rao[1], and Moturi Satyanarayana[2]

Abstract—In this paper, a capacitive coupled Dielectric Resonator Antenna (DRA) array with log periodic method is explored experimentally for X-band applications. The incidence free DRA series consists of seven rectangular Dielectric Resonators (DRs). For both DRA and MPA arrays, a series fed microstrip line was used. In this work, Log Periodic Microstrip Patch Antenna (LPMPA) and Log Periodic Dielectric Resonator Antenna (LPDRA) arrays have been designed and realized, and the performance characteristics such as return loss, VSWR, gain, and bandwidth are simulated and validated experimentally. The LPMPA antenna is in active state from 10.2 GHz to 12.9 GHz with a bandwidth of 2.7 GHz and a gain of 8.55 dB. The LPDRA antenna is in active state from 7.3589 GHz to 12.1060 GHz with an increased bandwidth of 4.7474 GHz and a gain value of 8.53 dB. The corresponding performance characteristics are presented at the end.

1. INTRODUCTION

Mobile and satellite communication systems in the age of smart devices require an intelligent structure with features such as wideband, moderate gain, small size, and multiband operation. The explosive expansion of wireless communication has led to the development of wideband and multiband antennas that provide more bandwidth for satellite and wireless data consumers.

The log-periodic technique is generally adopted to achieve bandwidth enhancement and good radiation characteristics. It is a very sophisticated and effective approach to achieve multi-frequency broadband antenna design. The class of antenna that has resulted is called a frequency-independent of log-periodic antenna.

In the early 1980s, Long et al. proposed a dielectric resonator can be used as a resonant antenna [1]. Their DRA offers several advantages, including high radiation efficiency, compact size, light weight, and flexibility in shape and feeding mechanism. Many new and existing wireless applications necessitate such features, which DRA characteristics provide. Capacitive coupled LPDRA is introduced to achieve significant multi-frequency wide bandwidth as well as radiation characteristics of the array, and a log-periodic technique has been implemented on DRA.

The dielectric resonator is typically built of a high permittivity material with $\varepsilon_r > 20$ and a Q factor of 50 to 500 [2–4]. When DRAs are in fundamental mode, they radiate like a magnetic dipole, regardless of their shape. By the $\frac{\lambda_0}{\varepsilon_r}$ connection, the dimension of DRA is related to the free space resonant wavelength. Because the dielectric constant has no effect on the radiation efficiency, a wide variety of dielectric constants can be employed.

Compared to a microstrip antenna, which only radiates through two narrow slots, DRA has the following advantages [3].

Received 23 November 2021, Accepted 8 April 2022, Scheduled 2 August 2022

* Corresponding author: Boddapallli Venkata Ramana (bvramana.bvcits@gmail.com).

[1] Department of Electronics and Communication Engineering, A U College of Engineering (A), Visakhapatnam, Andhra Pradesh, India. [2] Department of Electronics and Communication Engineering, MVGR College of Engineering (A), Vizianagaram, Andhra Pradesh, India.

- The DRA has a far broader bandwidth than a microstrip antenna since the entire construction radiates except the ground plane, which is simply a series of thin slots in a microstrip antenna. With around ten times the relative permittivity, about ten percent of the bandwidth could be reached.
- In addition, compared to a microstrip antenna, DRA has the potential to avoid surface waves, which is another appealing characteristic.
- The beautiful construction of a dielectric resonator antenna catches the attention of researchers since it does not suffer from metallic losses due to the absence of metal, resulting in a wide bandwidth, higher gain, and high efficiency.
- DRA constructions of various shapes, including hemisphere, triangle, cylinder, rectangle and others, are available on the market.
- Compared to rectangular and hemispherical DRAs, cylindrical DRAs are easier to design.
- The aspect ratio should be carefully maintained to achieve the optimum operating frequency and bandwidth.
- For linking energy to DRA, a variety of feeding techniques are used, including aperture, coaxial probe, conformal patch, and microstrip.
- In comparison to microstrip, coaxial probe and aperture-coupled feeding technologies are frequently utilized.
- Direct microstrip feeding approach is the most appropriate way for big antenna array design.
- According to research, a 17 percent bandwidth with 13.8 dB gain was attained between 5.05 GHz and 5.9 GHz utilizing a two-segment, eight-element DRA array antenna design.
- Similarly, between the frequencies of 3.5 GHz and 4.75 GHz, a cylindrical dielectric resonator (Alumina Ceramic) design obtained 27 percent bandwidth and 7.95 dB gain.

The use of X-band networking systems is much more popular these days. Tiny, light-weight antennas with low metallic losses and broadband capabilities are needed for satellite communication. For network engineering applications, the X-band frequency spectrum has been extended to about 7.0–11.2 GHz.

A variety of antenna arrays for X-band applications have been produced by a range of researchers. A phased array antenna installed on the Substrate-Integrated Waveguide (SIW) platform is explored for Right-Handed Circular Polarization (RHCP) by multi-layered production for X-band satellite communication. For S-band as well as X-band airborne applications, a dual-frequency, dual-polarization array antenna with a multilayer arrangement is created [5].

To conserve room on the feeding-line network, the two antenna arrays are on dissimilar layers, with the X-band array fed in sequence. Though, owing to the difficult circuitry arrangement, these antennas are seldom utilized. With the increased requirement for compactness and low metallic loses, a basic and compact DRA array architecture is sufficient to provide enhanced efficiency [6–8]. As a result, attempts were made to develop an alternate LPDRA array architecture that could have reasonable wideband output while still being cost-effective.

2. PROPOSED METHODOLOGY

An LPDRA array by a microstrip sequence feed line was built, fabricated, simulated, as well as tested in the real world. The array's elements are connected straight to the feed line, resulting in a highly dense as well as low-loss DRA array [9]. Using this sequence microstrip line feeding process, the array's volume and weight may be minimized. This array was designed for X-band applications, with low conductor loss and a broad bandwidth [10, 11].

2.1. Design and Geometry of Capacitive Coupled LPDRA Array

The LPDRA series is made up of seven Dielectric Resonators (DRs) with rectangular sections that are ordered in a log periodic series [12, 13]. Alumina 92 pct, a dielectric substrate with a low relative permittivity, is used to produce the DRs. Capacitive coupled microstrip line feeding powers the

collection. The DRs are straight attached to the microstrip feed line of $80 \times 2.5\,\text{mm}^2$. All of the resonators, including the feed line, are engraved on the similar FR4 substrate, which measures $\approx 80\,\text{mm}$ by 30 mm, has a relative permittivity of 4.4, with a thickness (T) of 1.6 mm. At the structure's end, the smallest resonators are fed into the sequence, and this is where the most radiation is released [14, 15]. An open circuit is used to terminate the feed thread at the other end. A limited ground plane with a distance of $74 \times 30\,\text{mm}^2$ is partially printed on the back side of the substrate [16]. Where there is an air space among the resonator as well as the ground plane, the LPDRA Q-factor is diminished. The array's essential architecture is the same as that of a regular log periodic array [17–21].

2.1.1. Design Dimensions of Capacitive Coupled LPDRA Array

Step by step procedure for the design of antenna

Step-1: Design a microstrip feed line on a substrate.

Step-2: Height of the substrate = 1.6 mm

Step-3: Length of the substrate above DRA = 80 mm

Step-4: Width of the substrate above DRA = 30 mm

Step-5: Height of the DRA = 3 mm

Table 1 shows the dimensions of capacitive coupled LPDRA array.

Table 1. Dimensions of capacitive coupled LPDRA array.

Dielectric Resonators	W (mm)	L (mm)
DR7	9.8	12.3
DR6	9.41	11.81
DR5	9.03	11.33
DR4	8.67	10.88
DR3	8.32	10.45
DR2	7.99	10.03
DR1	7.67	9.63

2.1.2. Geometry of Capacitive Coupled LPDRA Array

The resonators in the series are positioned with an 180° phase gap between them. The scaling factor (τ) is used to change the length (L), width (W), height (H), and spacing (S) among the resonating items. The value of relative spacing (σ) is normally selected from Carrel's map. For this design, the preferred value (τ) is 0.96. Figure 1 shows the front view of capacitive coupled LPDRA array. Figure 2 shows the side view of capacitive coupled LPDRA array.

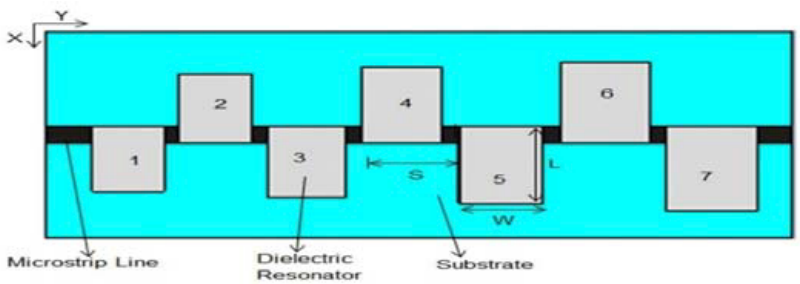

Figure 1. Front view of the capacitive coupled LPDRA array.

Figure 2. Side view of capacitive coupled LPDRA array.

From Figure 3 shown below, the components of a standard LP antenna are organized in rising order from the starting point to the ending point of the antenna, which is $2\alpha_d$ angle.

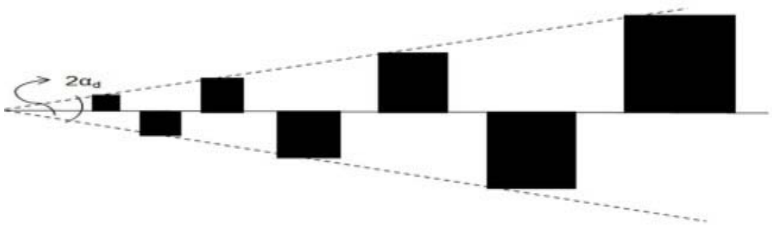

Figure 3. Typical LPA configuration.

2.1.3. Design Procedure

For a simple log-periodic antenna design, the scaling factor (τ) and relative spacing (σ) values are chosen directly from Carrel's table, where the maximum τ value cited is 1 [11]. Equation (1) represents the design parameter α_d. $10° \leq \alpha_d \leq 45°$ is the most typical α_d value. With the rise of α_d, the τ value begins to decline. Equations (2)–(4) are used to express the built bandwidth in terms of B_0 (desired bandwidth) as well as B_r (active area bandwidth) [22–27].

The design parameter α_d is described as follows:

$$\alpha_d = \tan^{-1}\left[\frac{1-\tau}{4\sigma}\right] \tag{1}$$

where 'σ' is the relative spacing.

The B_0 ratio of the maximum (f_H) to lowermost (f_L) frequency range given by equation is the desired bandwidth of the array (2)

$$B_0 = \frac{f_H}{f_L} \tag{2}$$

While the bandwidth of the system determines the lengths of the shortest and longest elements of the structure, the width of the active region depends on the specific design. Carrel has introduced a semi-empirical equation to calculate the bandwidth of the active region B_d related to α and τ.

In a Log periodic antenna, the designed bandwidth (B_d) must be higher than the desired bandwidth (B_0). Thus, it is expressed as follows.

$$B_d = B_O B_r \tag{3}$$

$$B_d = B_0\left[1.1 + 7.7\left(1-\tau^2\right)\cot\alpha\right] \tag{4}$$

where "α" is the phase angle.

The number of resonating elements (N_R) required for the design of LPDRA array can be obtained as given below

$$N_R = 1 + \left[\frac{l_n B_d}{l_n\,(1|\tau)}\right] \tag{5}$$

From one end to the other, the measurements of each DR part differ logarithmically. As the measurements of higher resonators (L, W, H, and S) are increased by τ, the higher resonator $m+1$

befalls m, and the smaller resonator m becomes $m-1$, implying that the sequence has similar electrical features at every frequencies associated by τ.

In this LPDRA array of series fed microstrip line, the measurements of the highest resonators are regularly compared to the lower frequency, which may be measured with Equations (6) to (8), where the lowest resonator's dimensions are related by the unit's maximum frequency.

The total length of the structure L, from the shortest ($l_{\min}$) to the longest ($l_{\max}$) element, is given by

$$L = \frac{\lambda_{\max}}{4} \tag{6}$$

$$\lambda_{\max} = \frac{c}{f_{\min}\sqrt{\varepsilon_r}} \tag{7}$$

where $\lambda_{\max}$ is the lowest frequency's wavelength ($f_{\min}$), c the speed of light in free space, and ε_r the dielectric resonator's comparative permittivity.

$$W = 0.8 \times L \tag{8}$$

$$W < S \leq \tau \cdot L \tag{9}$$

The spacing of neighboring resonators can be determined using Equation (9). Equation may be used to measure the measurements of the other dielectric components since the τ value for this design is $0.96(< 1)$ (5).

$$\tau = \frac{L_m}{L_m + 1} = \frac{W_m}{W_m + 1} = \frac{H_m}{S_m + 1} = \frac{S_m}{S_m + 1} \tag{10}$$

The dimensions (L, W, H, and S) of each dielectric resonator vary log periodically from one end to other. The basic design of the LPDRA is similar to that of a normal log-periodic array. The proposed LPDRA consists of seven DRs of different lengths, widths, and spacing — excited by a series of microstrip line feeding. Bandwidth is improved to Log periodic dielectric Resonator Antenna when Log periodic microstrip patch antenna and Log periodic dielectric Resonator Antenna are compared.

The dielectric waveguide model is used to study the rectangular DRA [8]. If the DRA is on a land plane, TE modes are enabled. The fundamental mode's resonant frequency, TE111, is determined using the equations below.

$$f_o = \frac{c}{2\pi\sqrt{\varepsilon_r}}\sqrt{k_x^2 + k^2{}_y + k^2{}_z} \tag{11}$$

$$k_x = \frac{\pi}{a}, \quad k_z = \frac{\pi}{2b}, \quad d = \frac{2}{k_y}\tanh\left(\frac{k_{y0}}{k_y}\right), \quad k_{y0} = \sqrt{k_x^2 + k_z^2} \tag{12}$$

where ϵ_r is the resonator's proportional dielectric constant as well as is the resonator's dielectric constant.

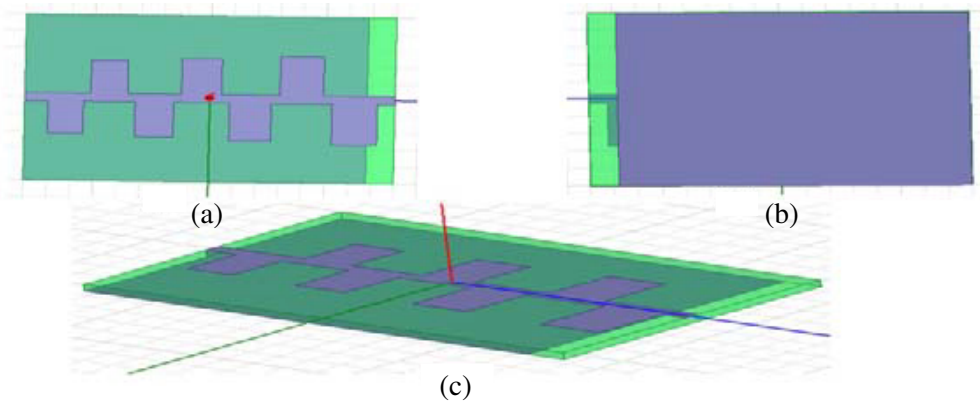

Figure 4. Structures of capacitive coupled log periodic patch antenna. (a) Top view. (b) Back view. (c) Side view.

The largest element in the LPDRA has measurements of 12.3 mm length, 9.8 mm width, and 3 mm height, by middle to center spacing (S) of 11.3 mm between two resonators. As seen, the measurements of other DR components are scaled by. The array's total measurements are $80 \times 30\,\text{mm}^2$. This antenna architecture can be used to obtain broadside radiation patterns and a small bandwidth with high gain.

Designed structures of capacitive coupled log periodic patch antenna are shown in Figure 4. In that, Figure 4(a) shows the top view, Figure 4(b) the back view, and Figure 4(c) the side view.

Similarly, designed structures of the capacitive coupled log periodic DRA antenna are shown in Figure 5. In that, Figure 5(a) shows the top view, Figure 5(b) the back view, and Figure 5(c) the side view.

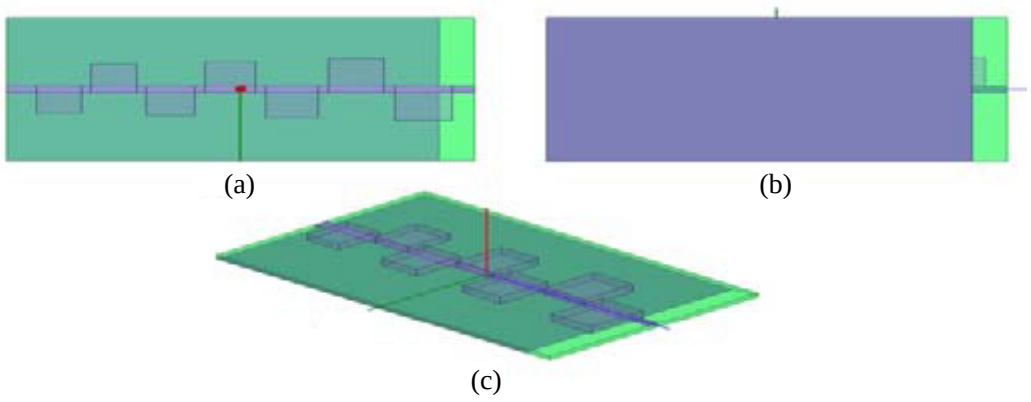

Figure 5. Structures of capacitive coupled log periodic DRA. (a) Top view. (b) Back View. (c) Side view.

2.2. Fabrication of Capacitive Coupled Antenna

Figure 6 shows images of a capacitive coupled patch antenna that has been fabricated with 7 elements. Each patch antenna element grows logarithmically from one end to the other.

Figure 7 shows a fabricated array capacitive coupled without DRA, while Figure 8 shows an

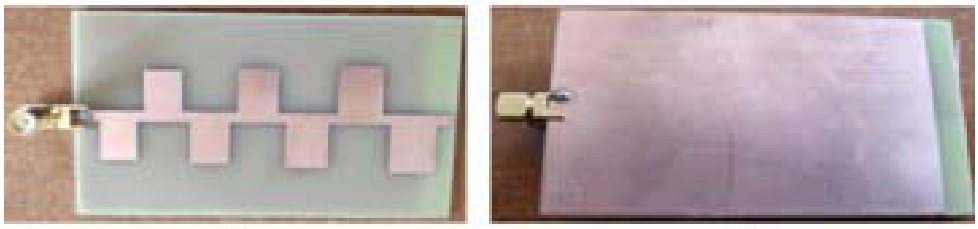

Figure 6. (a) Patch antenna front view. (b) Patch antenna back view.

Figure 7. (a) Front view of array without DRA. (b) Back view of an array without DRA.

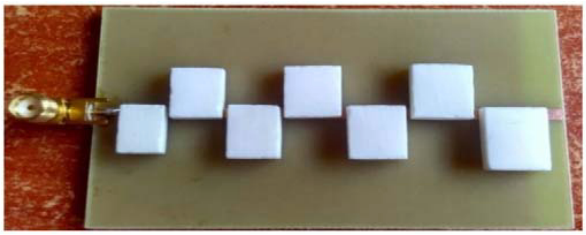

Figure 8. Front view of an array with DRA.

array with DRA. From one end to the other, the measurements of each patch part element differ logarithmically.

2.3. Measurement Setup for Fabricated Antennas Using Network Analyzer

The below figures show the testing bench setup for network analyzer based fabricated antenna. In that, Figure 9(a) shows the back view of experimental setup for taking the measurement results of fabricated capacitive coupled array antenna, and Figure 9(b) shows the front view of capacitive coupled patch.

(a) (b)

Figure 9. (a) Back view of capacitive patch. (b) Front view of capacitive patch.

Figure 10 shows the side view of capacitive patch. Similarly, the Figure 11(a) shows the back view of capacitive coupled DRA, and Figure 11(b) shows the front view of capacitive DRA. Figure 12 shows the side view of the capacitive DRA.

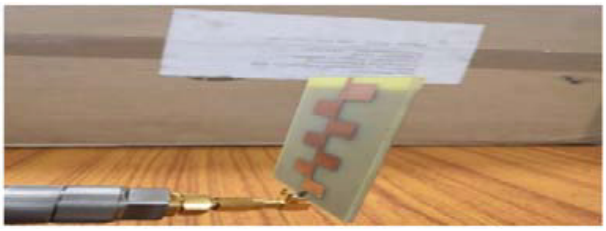

Figure 10. Side view of capacitive patch.

3. RESULTS AND DISCUSSION

For X-band communication systems, a frequency independent DRA array prototype was planned and realized. The following subsections go through the findings centered on simulated using the HFSS. The

(a) (b)

Figure 11. (a) Back view of capacitive DRA. (b) Front view of capacitive DRA.

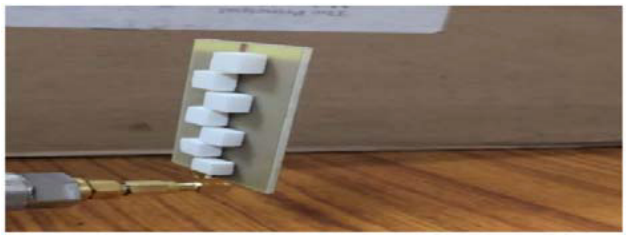

Figure 12. Side view of capacitive DRA.

simulated results of the array are in terms of return loss, VSWR, radiation pattern, gain, bandwidth, and calculated evidence. The simulated VSWR result is compared favorably with the physically measured values. The bandwidth of LPDRA is 7.3589–12.10 GHz, which is the desired frequency range for X band applications. The gain, bandwidth, VSWR, and radiation performance of the DRA can be modified using a log-periodic array instead of a basic shaped DRA.

3.1. Return Loss

Figure 13 shows the simulated response of return loss for capacitive coupled DRA antenna is −30.39, and the measured response of return loss is −30.40.

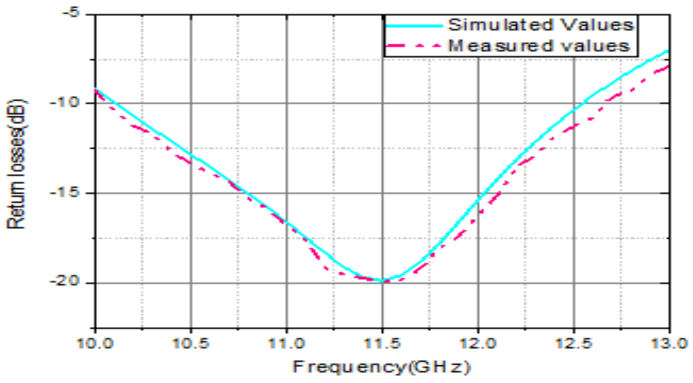

Figure 13. Return loss of capacitive coupled patch antenna.

Similarly, Figure 14 shows the simulated response of return loss for capacitive coupled DRA antenna which is −34.53, and the measured response of return loss is −35.1. Figure 15 shows the comparison of the return losses between capacitive coupled patch and DRA.

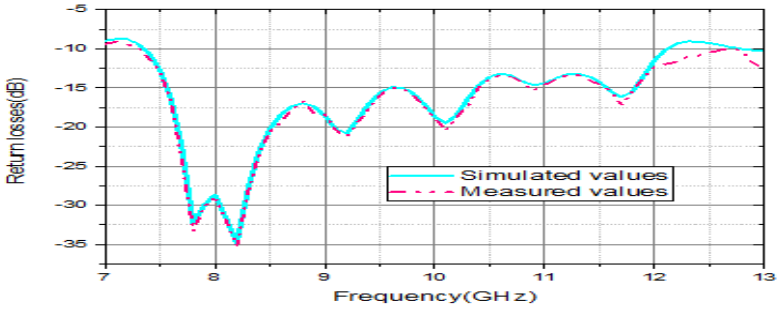

Figure 14. Return loss of capacitive coupled DRA.

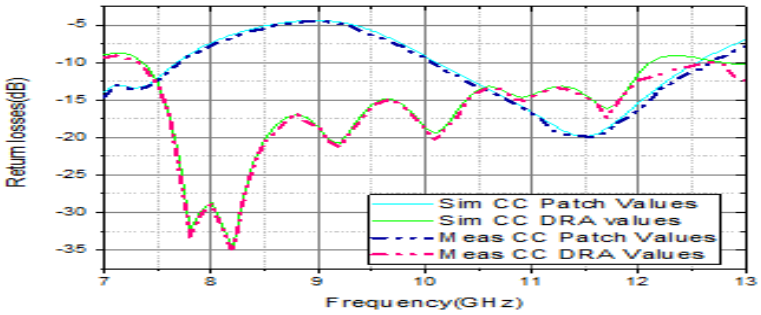

Figure 15. Comparison of return loss between capacitive coupled patch and DRAs.

3.2. VSWR

Figure 16 shows the simulated response VSWR of a capacitive coupled patch antenna is 1.25, and measured response of VSWR is 1.25.

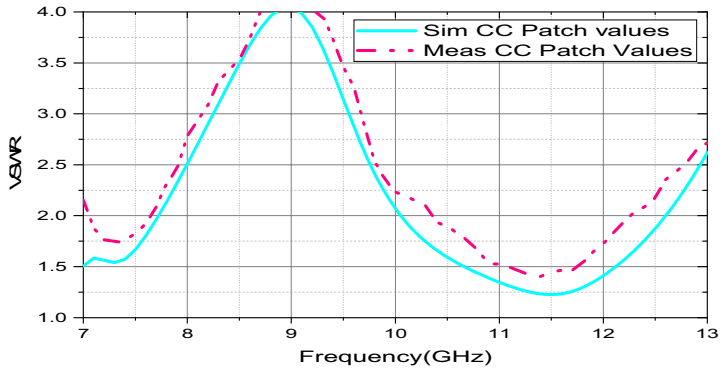

Figure 16. VSWR of capacitive coupled patch antenna.

Similarly, Figure 17 shows the simulated response of VSWR for capacitive coupled DRA antenna which is 1.4, and measured response of VSWR is 1.11. Figure 18 shows the comparison of VSWRs between capacitive coupled patch and DRA.

3.3. Gain and Frequency

Figure 19 shows that the simulated response of gain versus frequency curve for capacitive coupled patch antenna is 8.55 dB at 9.8 GHz, and measured response of gain is almost similar.

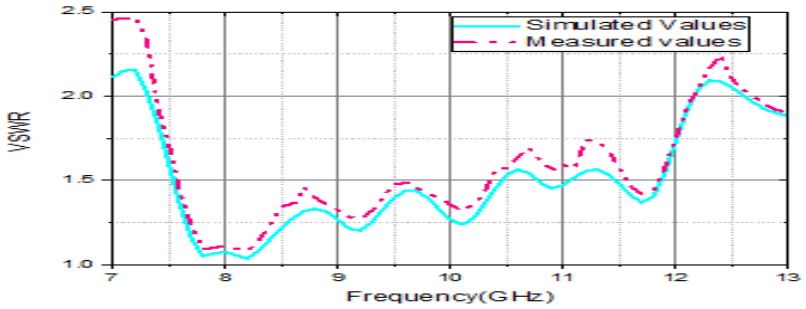

Figure 17. VSWR of capacitive coupled DRA.

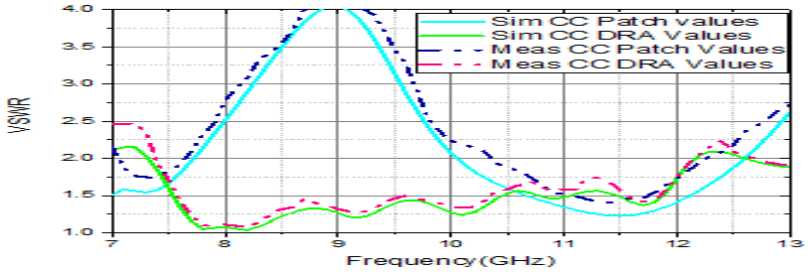

Figure 18. Comparison of VSWR of between capacitive coupled patch and DRAs.

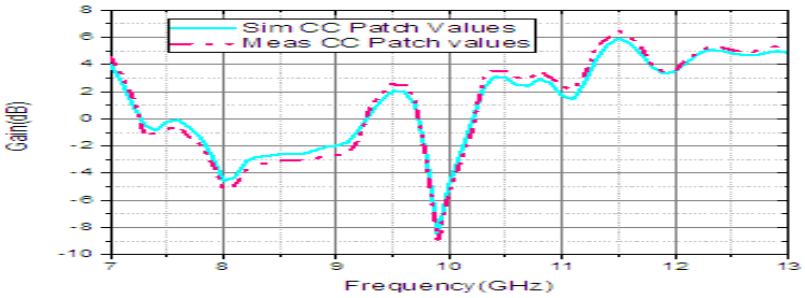

Figure 19. Gain versus frequency curve of capacitive coupled patch antenna.

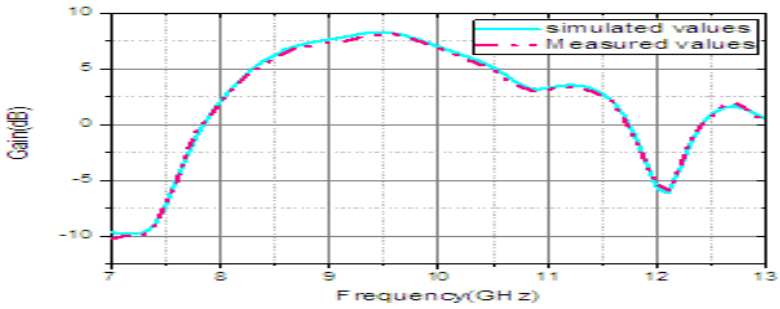

Figure 20. Gain versus frequency curve of capacitive coupled DRA.

Similarly, Figure 20 shows that the simulated response of gain versus frequency curve for capacitive coupled patch antenna is 8.53 dB at 9.6 GHz, and measured response of Gain is almost similar. Figure 21 shows the comparison of gain versus frequency curve between capacitive coupled patch and DRA.

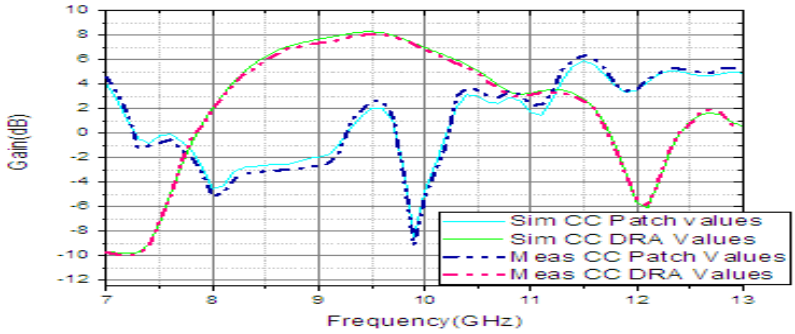

Figure 21. Comparison of gain versus frequency curve between capacitive coupled patch and DRAs.

3.4. Polar Plot

A polar diagram is a graph that displays the magnitude of a response in both directions. The 3D polar plot of a capacitive coupled patch antenna is seen in Figure 22. At resonant frequency the observed gain is 8.55 dB.

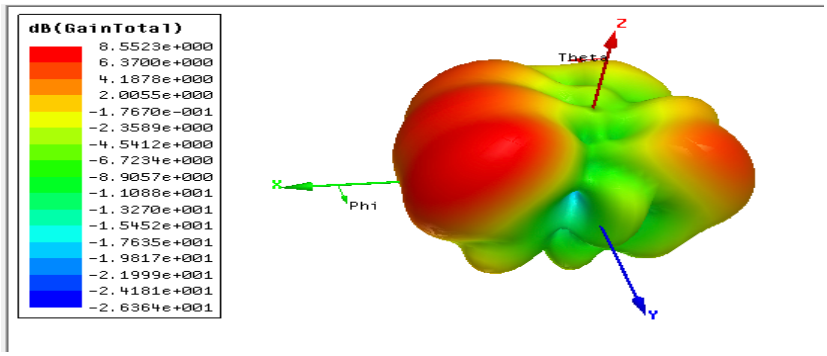

Figure 22. 3D polar plot of capacitive coupled patch antenna.

The 3D polar plot for a capacitive coupled DRA is depicted in Figure 23. At resonant frequency the observed gain is 8.53 dB.

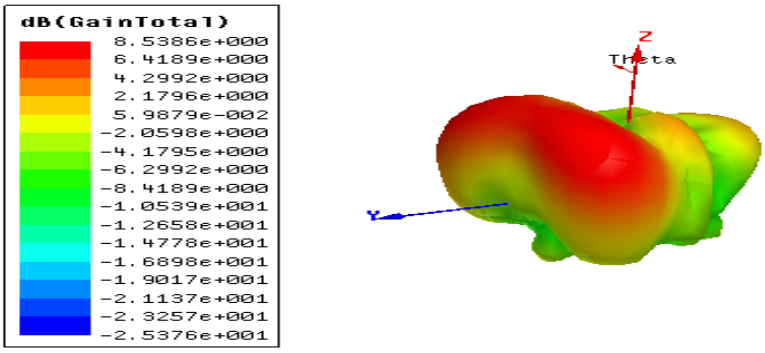

Figure 23. 3D polar plot of capacitive coupled DRA antenna.

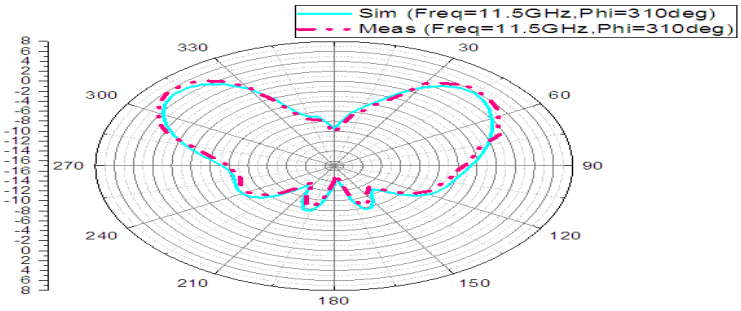

Figure 24. Radiation pattern of capacitive coupled patch antenna.

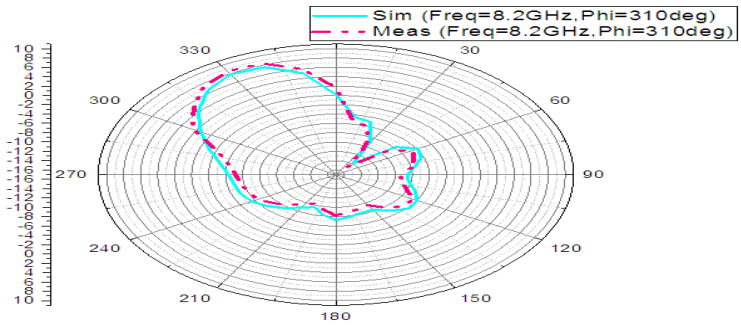

Figure 25. Radiation pattern of capacitive coupled DRA antenna.

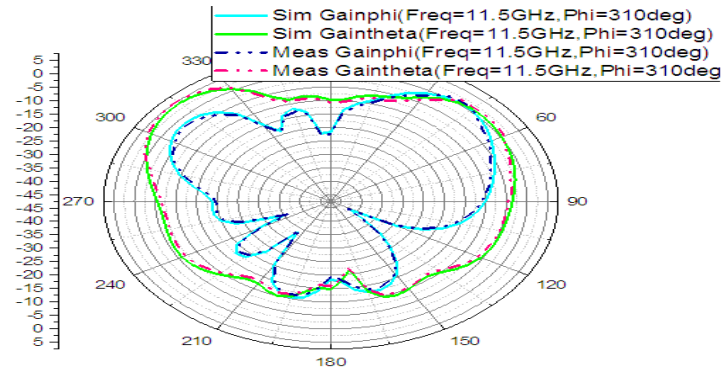

Figure 26. Simulated and measured co-polarization and cross polarization of capacitive coupled patch antenna.

3.5. Radiation Pattern

The radiation pattern describes the behaviour of antenna direction. Figure 24 shows the radiation distribution of a capacitive coupled patch antenna, simulated and measured radiation patterns at resonant frequency which is 11.5 GHz. Figure 25 shows the radiation distribution of a capacitive coupled DRA antenna. We simulated and measured radiation patterns at a resonant frequency of 8.2 GHz.

3.6. Co-Polarization and Cross-Polarization

Co-polarization: The polarization of the wave that would be radiated by the antenna that is needed. Cross-polarization (X-pw) is the orthogonal radiation of a desired wave polarization (the polarization of above wave). The co-polarization and cross-polarization of a capacitive coupled patch antenna are seen in Figure 26. Figure 27 depicts the capacitive paired DRA's co-polarization and cross-polarization.

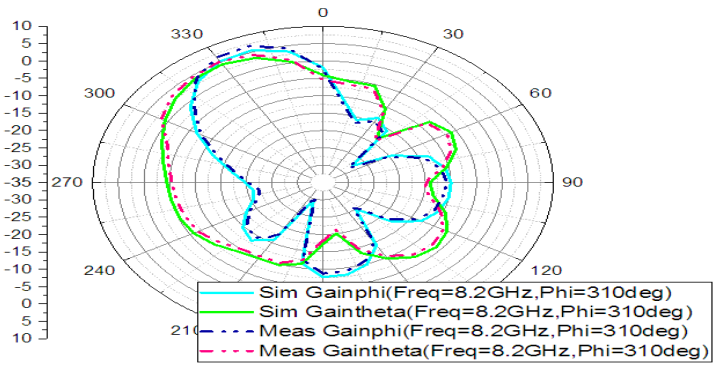

Figure 27. Simulated and measured co-polarization and cross polarization of capacitive coupled DRA antenna.

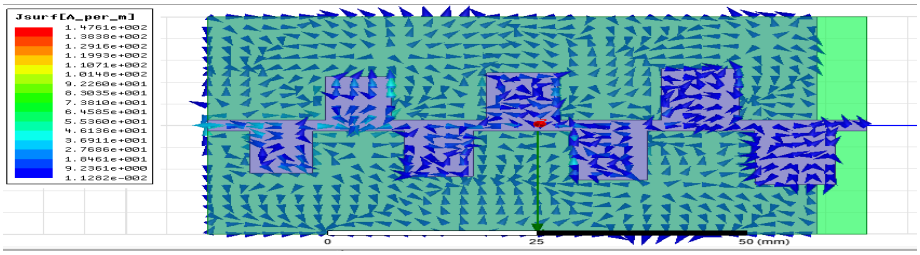

Figure 28. Current distribution of capacitive coupled patch antenna.

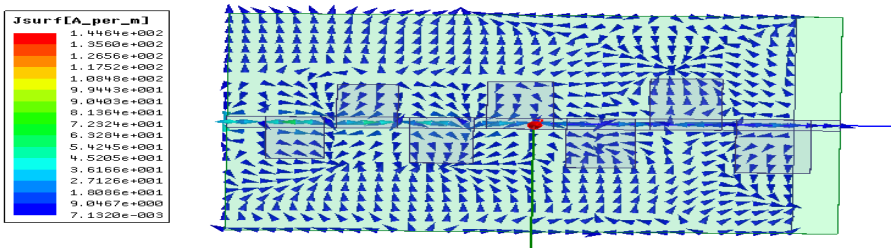

Figure 29. Current distribution of capacitive coupled DRA antenna.

3.7. Current Distribution

Figure 28 shows the surface current distribution of capacitive coupled patch antenna and specifies different modes of propagation as well as various resonant frequencies. Similarly, Figure 29 shows the current distribution for capacitive coupled DRA. Table 2 shows the comparison between patch and DRAs. Table 3 shows the comparison of the proposed method to another Log periodic DRA.

Table 2. Comparison between patch and DRA antennas.

Case	Operating Band	Return Loss	VSWR	Bandwidth	Gain	%Bandwidth
Capacitive coupled LPMPA	10.2 GHz to 12.9 GHz	−30.3920	1.08	2.7 GHz	8.55 dB	23.53%
Capacitive coupled LPDRA	7.3589 GHz to 12.1060 GHz	−34.5325	1.407	4.747 GHz	8.53 dB	51.6%

Table 3. Comparison of the proposed capacitive coupled log periodic DRA with other log periodic DRA.

Ref.	Frequency	Design	Return loss	Gain (dB)	Bandwidth	%Bandwidth
[19]	3.1 GHz to 13.83 GHz	Wideband Printed Log-Periodic Dipole Antenna	22.4119 dB	6.4	10.67 GHz	33.84%
[20]	2.66 GHz–3.4 GHz	Design of Log Periodic Inset Fed Micro strip Patch Antenna for S-Band Applications	17.7 dB	4.74	0.74 GHz	24.6
[21]	4.80 GHz to 7.06 GHz	Design of Logarithmic periodical Di-electric Resonator Array for Wide Band Implementations	−18.8722 dB	5.7	9–10 GHz	38.11%
[22]	8.4089 GHz to 12.550 GHz	Aperture Coupled Log periodic DRA Using X band applications	−27.4744 dB	6.076	4.14 GHz	45.19
[23]	7.575 GHz to 8.64 GHz	Wide-Band Log-Periodic Micro strip Antenna with Defected Ground Structure for C-Band Applications	−26.23 dB	8.73	0.91 GHz	48.1
Proposed antenna array	7.3589 GHz to 12.1060 GHz	Capacitive coupled LPDRA	−34.5325	8.53 dB	4.747 GHz	51.6%

4. CONCLUSION

In this research work, wideband log periodic LPMPA and LPDRA have been designed. These two antennas are operated by a series-fed microstrip line, and the patches in LPMPA and the resonators in LPDRA are directly coupled to the feed line for minimizing the array losses. From results, it is shown that the LPMPA is in active state from 10.2 GHz to 12.9 GHz with a bandwidth of 2.7 GHz and a gain of 8.55 dB. Also, the LPDRA is in active state from 7.3589 GHz to 12.1060 GHz and exhibits a bandwidth of 4.7474 GHz with a gain of 8.45 dB. The implementations of dielectric resonators instead of patches have increased the percentage bandwidth from 23.53% to 51.6%. The proposed LPDRA array is well designed and suitable for X-band satellite communication systems and RADAR applications with good performance.

REFERENCES

1. Long, S. A., M. W. McAllister, and L. C. Shen, "The resonant dielectric cavity antenna," *IEEE Transactions on Antennas and Propagation*, Vol. 31, No. 3, 406–412, March 1983.
2. Upadhyaya, T. and K. Pandya, "A rieview on dielectric resonator antenna," *1ST International Conference on Automation in Industries (ICAI)*, 106–109, 2016.
3. Vahora, A. and K. Pandya, "Implementation of cylindrical dielectric resonator antenna array for Wi-Fi/wireless LAN/satellite applications," *Progress In Electromagnetic Research M*, Vol. 90, 157–166, 2020.
4. Liu, Y.-T., K. W. Leung, J. Ren, and Y.-X. Sun, "Linearly and circularly polarized filtering dielectric resonator antennas," *IEEE Transactions on Antennas and Propagation*, Vol. 67, No. 6, 3629–3640, 2019.

5. Wang, M. and Q.-X. Chu, "A wideband polarization-reconfigurable water dielectric resonator antenna," *IEEE Antennas and Wireless Propagation Letters*, Vol. 18, No. 2, 402–406, 2019.
6. Kumari, R. and S. K. Behera, "Capacitive coupled frequency independent dielectric resonator antenna array for X-band applications," *IETE Journal of Research*, 2019, doi: 10.1080/03772063.2019.1600438.
7. Petosa, A., *Dielectric Resonator Antenna Handbook*, 1–3, Artech House Publishers, Norwood, 2007.
8. Luk, K. M. and K. W. Leung, *Dielectric Resonator Antennas*, 1–45, Research Studies Press Ltd., Hertfordshire, 2002.
9. Mongia, R. K. and P. Bhartia, "Dielectric resonator antennas — A review and general design relations for resonant frequency and bandwidth," *International Journal of Microwave and Millimeter-Wave Computer-Aided Engineering*, Vol. 4, No. 3, 230–247, Jul. 1994.
10. Gao, Y., Z. Feng, and L. Zhang, "Compact dielectric resonator on-patch antenna with bandwidth enhancement," *Microwave and Optical Technology Letters*, Vol. 54, No. 1, 66–71, Jan. 2012.
11. Balanis, C. A., *Antenna Theory Analysis and Design*, John Wiley & Sons, Inc., Hoboken, New Jersey, 2005.
12. Luk, K.-M. and K.-W. Leung, *Dielectric Resonator Antennas*, Research Studies Press Ltd., England, 2003.
13. Petosa, A. and A. Ittipiboon, "Dielectric resonator antennas — A historical review and the current state of the art," *IEEE Antennas and Propagation Magazine*, Vol. 52, No. 5, 91–116, 2010.
14. Chen, S. Y., P. H. Wang, and P. Hsu, "Uniplanar log-periodic slot antenna fed by a CPW for UWB applications," *IEEE Antennas and Wireless Propagation Letters*, Vol. 5, No. 1, 256–259, 2006.
15. Zhai, G. H., W. Hong, K. Wu, and Z. Q. Kuai, "Wideband substrate integrated printed log periodic dipole array antenna," *IET Microwave Antennas and Propagation*, Vol. 4, No. 7, 899–905, 2010.
16. Jardon-Aguilar, H., J. A. Tirado-Mendez, R. Flores-Leal, and R. Linares-Miranda, "Reduced log-periodic dipole antenna using a cylindrical-hat cover," *IET Microwave Antennas and Propagation*, Vol. 5, No. 14, 1697–1702, Nov. 2011.
17. Yu, C., W. Hong, L. Chiu, G. Zhai, C. Yu, W. Qin, and Z. Kuai, "Ultra wideband printed log-periodic dipole antenna with multiple notched bands," *IEEE Transactions on Antennas and Propagation*, Vol. 59, No. 3, 725–732, Mar. 2011.
18. Kumari, R. and S. K. Behera, "Investigation on log periodic dielectric resonator antenna array for Ku band applications," *Taylor & Francis, Electromagnetics*, Vol. 34, 19–33, 2014.
19. Kumari, R. and S. K. Behera, "Nine element frequency independent dielectric resonator array for X-band applications," *Microwave and Optical Technology Letters*, Vol. 55, 400–403, 2013.
20. Kumari, R. and S. K. Behera, "Wideband log periodic dielectric resonator array with overlaid micro strip feed line," *IET Microwave Antennas and Propagation*, Vol. 7, 582–587, 2013.
21. Kumari, H. R., "Investigations on possible realization of log periodic dielectric resonator antennas," National Institute of Technology, Rourkela, 2013.
22. Balanis, C. A., *Antenna Theory: Analysis and Design*, 619–637, John Wiley & Sons, New York, 2005.
23. Ramana, B. V., P. Mallikarjuna Rao, and M. Satyanarayana, "Wideband printed log-periodic dipole antenna," *Jour. of Adv. Research in Dynamical & Control Systems*, Vol. 11, No. 1, 39–47, 2019.
24. Ramana, B. V., M. Satyanarayana, and P. Mallikarjuna Rao, "Design of log periodic inset fed microstrip patch antenna for S-band applications," *Proceedings of the Fifth International Conference on I-SMAC (IoT in Social, Mobile, Analytics and Cloud) (I-SMAC)*, IEEE, Palladam, India, 2021.
25. Ramana, B. V., M. Satyanarayana, and P. Mallikarjuna Rao, "Design of logarithmic periodical dielectric resonator array for wide band implementations," *International Journal of Engineering and Advanced Technology*, Vol. 8, No. 2S2, 219–226, Jan. 2019.
26. Pimpalgaonkar, P., T. Upadhyaya, K. Pandya, M. R. Chaurasia, and B. Raval, "A review on dielectric resonator antenna," *ICAI 2016*, 2016.

27. Upadhyay, K. K., A. Agrawal, and M. Misra, "Wide-band log-periodic microstrip antenna with defected ground structure for C-band applications," *Progress In Electromagnetics Research C*, Vol. 112, 127–137, 2021.